A mesomorphic amphiphilic phthalocyanine derivative used for the functionalization of the grid surface of a field effect transistor

Angela Sastre, Pierre Bassoul, Christian Fretigny, Jacques Simon,* Jean-Paul Roger and Thierry Thami

Laboratoire de chimie inorganique matériaux moléculaires, ESPCI, (CNRS UPRESA 7071), 10, rue Vauquelin, 75231 Paris cedex 05, France

A phthalocyanine subunit substituted with four hydroxy- and four methoxy-terminated polyoxyethylene sidechains has been synthesized. Optical microscopy and X-ray diffraction at small angles demonstrate the formation of a birefringent non-crystalline phase. The reaction of the terminal hydroxy groups with methacryloyl chloride affords an amphiphilic photopolymerizable phthalocyanine derivative. This latter has been reacted with the grid surface of a field effect transistor (FET) previously treated with (trimethoxysilyl)propyl methacrylate. The photo-copolymerized membrane has been shown to be approximately 360 Å thick by atomic force microscopy (AFM). The covalently linked polyoxyethylene phthalocyanine derivative has been used as an ion complexing membrane in an ion selective field effect transistor (ISFET). The ISFET characteristics have been determined in water and in a methanol–water mixture (90 : 10; v : v) for Na^+ and K^+. The pH sensitivity of the device has also been measured. The experimental results have been compared with theoretical ones. The model allowed us to determine the total number of binding sites (N_{TOT}) and the corresponding ion–site complexation constants.

Fonctionnalisation d'une grille de transistor à effet de champ par un dérivé amphiphile de phtalocyanine formant des mésophases. Un dérivé de phtalocyanine substitué par huit chaînes polyoxyéthylènes—quatre d'entre elles se terminant par un groupe hydroxy, quatre autres par un groupe méthoxy—a été synthétisé. Des observations en microscopie optique et des mesures de diffraction des rayons X aux petits angles démontrent la formation de mésophases biréfringentes avec ce composé. Les groupes terminaux hydroxy sont ensuite transformés en ester méthacrylique afin d'obtenir un dérivé de phtalocyanine photopolymérisable. Une grille de transistor à effet de champ en silice a été préalablement traitée à l'aide de (triméthoxysilyl)propylméthacrylate. Ceci a permis de greffer le dérivé de phtalocyanine sur la surface de SiO_2 par photopolymérisation. La membrane ainsi obtenue fait environ 360 Å d'épaisseur. Celle-ci fut déterminée à l'aide d'un microscope à force atomique. Le dispositif précédent a été utilisé pour détecter et titrer des ions sodium et potassium fonctionnant ainsi comme un transistor à effet de champ sensible aux ions. Ses caractéristiques ont été déterminées dans l'eau et dans un mélange méthanol–eau (90 : 10; v : v). Les modifications dues à des changements de pH ont été mesurées. Les résultats expérimentaux ont pu être modélisés grâce à une approche déjà décrite. Celle-ci nous a permis de calculer à la fois le nombre total de sites complexants et la constante de stabilité site–cation.

The grid of field effect transistors may be functionalized in order selectively to complex metallic ions or bind protons.[1–4] The bound ions may in turn influence the intensity of the source-to-drain current (Fig. 1).

Phthalocyanine (Pc) subunits substituted with paraffinic[5,6] or polyoxyethylene[7,8] chains have been shown to form columnar liquid crystalline phases by segregation of the central rigid core from the flexible side chains. On the other hand, polyoxyethylene is well-known to yield fairly high ionic conductivities when electrolytes are added in the material.[9,10] Recently, such an ionic conductivity has been demonstrated for a mesophase derived from polyoxyethylene-substituted phthalocyanines.[11] Crown-ether-substituted phthalocyanines have also been used to functionalize the grid of ISFETs.[12]

In the present article, the synthesis of a phthalocyanine subunit substituted with four hydroxy- and four methoxy-terminated polyoxyethylene side chains is described (Fig. 2). Under mild conditions, the terminal hydroxy groups may be transformed into the corresponding methacryloyl derivatives. The amphiphilic phthalocyanine thus obtained may be reacted with the silica surface of the ISFET grid previously treated with (trimethoxysilyl)propyl methacrylate as schematically pictured in Fig. 3. Because of the strong segregation tendency of the rigid hydrophobic Pc core and of the hydrophilic polyoxyethylene side chains, a more or less structured material is expected in the monomeric and polymeric phases of the amphiphilic phthalocyanine.

The polymeric membrane linked to the grid surface can extract more or less selectively ions present in aqueous or alcoholic media, thus acting as the membrane of an ISFET.

Results and Discussion

Materials and methods

Synthesis of 1. The chemical pathway used for the synthesis of the unsymmetrically octasubstituted phthalocyanines **1a** and **1b** is shown in Scheme 1. Dibromocatechol[13] **2** was treated with 1-chloro-8-methoxy-3,6-dioxaoctane in the presence of sodium hydroxide to give **3** in 41% yield. 4-Hydroxy-5-[9-methoxy-1,4,7-trioxanonane]phthalonitrile **4** was prepared from **3** *via* a Rosenmund-von Braun reaction;[14] the excess of CuCN was removed by treatment with $FeCl_3$ under acidic conditions (yield 36%). 1-Chlorotriethylene glycol was reacted with **4** in the presence of K_2CO_3 in DMSO to yield **5**

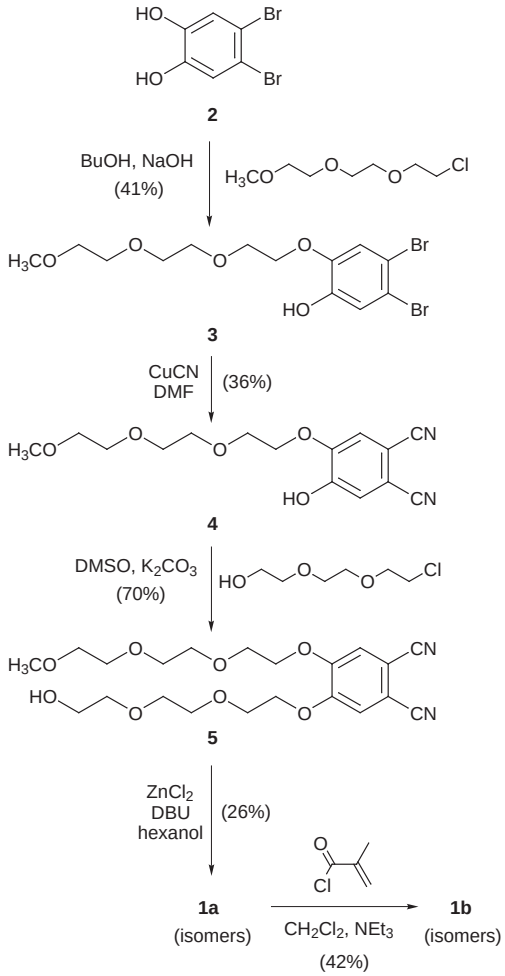

Scheme 1 Chemical pathway used to synthesize the amphiphilic-functionalized phthalocyanine derivatives

in 70% yield. This latter compound was reacted with $ZnCl_2$ and 1,8-diazabicyclo[5.4.0]undec-7-ene (DBU) in 1-hexanol under reflux to afford the zinc phthalocyanine derivative **1a** constituted of four positional isomers (yields 26%).

Starting from dibromocatechol, the overall yield to obtain **1a** is about 2.7% and 1.1% for **1b**. Microanalyses and other physicochemical characterizations (^{1}H NMR, mass spectrometry, UV/VIS spectrum) are in agreement with the proposed structures.

1a is highly soluble in a wide variety of solvents from $CHCl_3$ to H_2O. Remarkably, traces of impurities (probably dichlorocarbene) present in $CDCl_3$ oxidize **1a** into a brownish-red paramagnetic compound after some time.

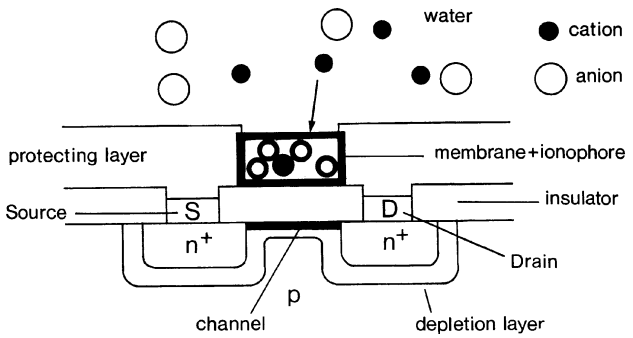

Fig. 1 Schematic representation of an ion selective field effect transistor (ISFET). From ref. 12 with permission of the publisher

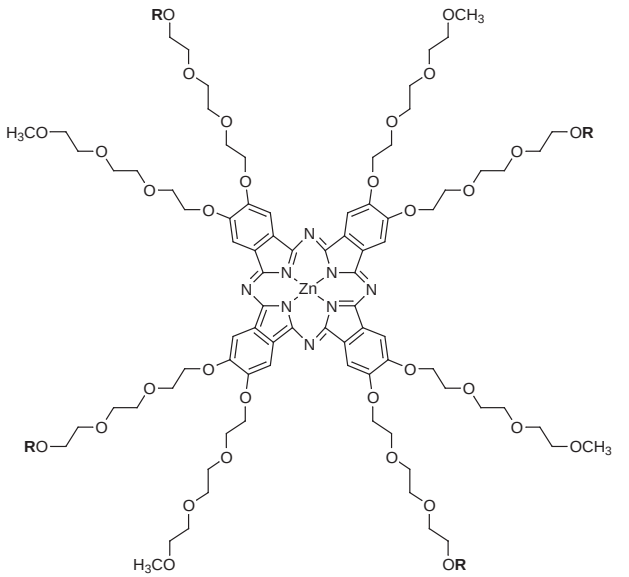

Fig. 2 Chemical formula of the phthalocyanine substituted with polyoxyethylene sidechains (the real compound is a mixture of isomers). **1a**: R = H; **1b**: R = —$COC(CH_3)$=CH_2

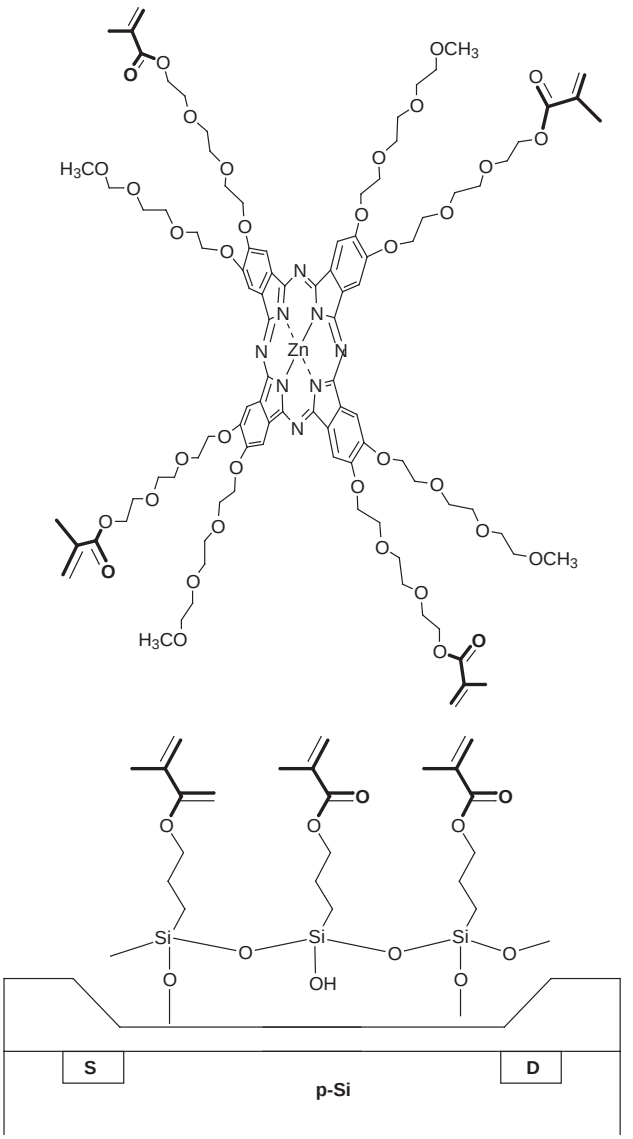

Fig. 3 Photoinduced copolymerization between the amphiphilic phthalocyanine substituted with methacrylate moieties and the silica surface of the grid functionalized *via* a treatment with (trimethoxysilyl)propyl methacrylate (sizes not relative)

Mesomorphic properties. The mesomorphic properties of **1a** and **1b** have been determined by crossed polarizer light microscopy, differential scanning calorimetry (DSC) and X-ray diffraction at small angles.

By optical microscopy, compound **1a** is birefringent with no transition up to 230–250 °C, where a fluid isotropic liquid appears. When the isotropic liquid is cooled down at a moderate rate (2 °C min^{-1}) a texture is observed that is closely related to the one observed for nematic mesophases derived from dimeric phthalocyanine complexes;[15] the same texture was observed even at room temperature. However, no transition is observed by DSC. The use of the mixture of four positional isomers probably leads to very broad DSC peaks that are undetectable. It seems, however, that a liquid crystalline state is present at room temperature. X-Ray diffraction at small angles shows one fairly narrow peak at 23 ± 1 Å and a halo at 4.2 Å. This is compatible with a previously described nematic-like phase.[15]

1b, which is substituted with four methacrylate groups, has also been studied by optical microscopy and DSC but no clear results could be obtained because of more or less complete polymerization during the physicochemical studies.

Synthesis and characterization of the membrane linked to the ISFET grid. The ISFET used was fabricated at the Centre Interuniversitaire de MicroElectronique (CIME). The main characteristics have been previously described:[12,16] substrate *p*-Si; channel length and width: 20 and 500 μm, respectively; SiO_2 thickness: 900 Å.

The silica surface of the grid was first treated with a sulfochromic mixture to remove all organic impurities and to increase the density of silanol groups.[17] Under these conditions, approximately 10^{14} silanol groups per cm^2 are obtained on the grid surface (1 every 100 $Å^2$).

The silanization with (trimethoxysilyl)propyl methacrylate was achieved using a 10% solution (v : v) of this compound in toluene–water (99.5 : 0.5) for 4 h under reflux. In this way a single layer of the silyl derivative is obtained (functionalized ungrafted device). The thickness of the organic layer has been determined by ellipsometry and is in the range of 6–12 Å, depending on the experiment.[12] This value is in agreement with the length of the silylpropyl methacrylate moiety derived from molecular models.

The membrane was obtained by copolymerization of the methacrylate groups covalently linked to the surface with the amphiphilic methacrylate phthalocyanine **1b** (grafted device). 2,2′-Dimethoxyphenylacetophenone (DMPA) was used as photoinitiator (see *Experimental*). The resulting film thickness was determined from UV/VIS spectra on glass slides treated under exactly the same conditions. The thin film optical spectrum shows two peaks at 639 and 678 nm, which were previously assigned to the dimeric (or aggregated) and monomeric phthalocyanine forms, respectively.[18] Taking the absorption coefficients in solution previously measured,[18] a proportion of 80% dimer for 20% of monomer may be estimated in the membrane. This leads to an approximate thin film thickness of 200 Å assuming a density of 1.44 g cm^{-3} as calculated from X-ray studies on mesophases.[11] Ellipsometry measurements lead to approximately twice this last value (355 Å). The topological properties of the membrane have then been determined by atomic force microscopy (AFM) (Fig. 4) to clarify this point.

AFM images show that the material is distributed inhomogeneously on the substrate. Numerous holes, having diameters of around 2000 Å, are present in the film. The 'walls' between the holes are approximately 360 Å high and their top surface is nearly flat (±3 Å). The wavelength used in ellipsometry is around 5000 Å: the 'holes' present in the layer are therefore expected to lead to strong multireflection and diffusion effects. The surface of the top layer is the only one observable by

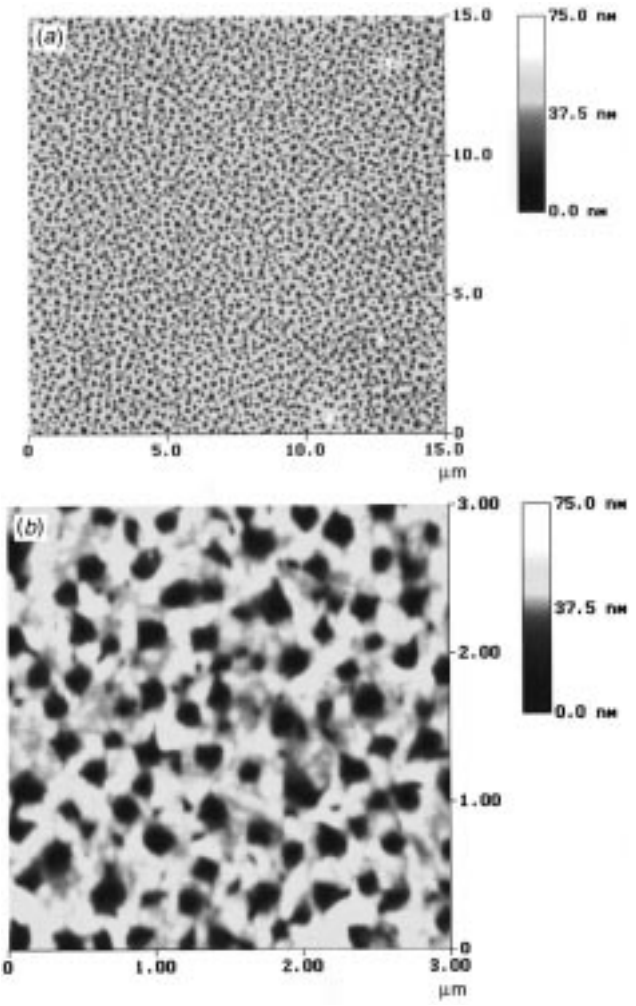

Fig. 4 AFM image of the amphiphilic phthalocyanine membrane: (*a*) 15 × 15 μm; (*b*) 3 × 3 μm

ellipsometry and no averaging between the different levels occurs. Taking into account the inhomogeneous distribution of the organic matter, the AFM thickness of 360 Å is therefore in perfect agreement with the one measured by ellipsometry (355 Å) and in accordance with the UV/VIS results for which an average value is measured (200 Å).

Further investigations have been carried out by electron diffraction. A film of amorphous carbon was deposited under vacuum on the membrane, which was then removed from the silica surface by using a solution of potassium hydroxide. Diffraction showed a single extremely narrow ring around 21 ± 0.5 Å, which can be due to the previously described 'Pincement de Skoulios'.[19] No indication of a structural arrangement of the columns could be detected. The ring observed seems to demonstrate the presence of columns but not periodically organized.

ISFET

Model used. The modified site-binding model[20,21] has been used to interpret our results. In this model the cations are considered to be complexed at defined binding sites on the grid surface, generating an excess positive charge expressed as σ_0 (in C cm^{-2}) with a corresponding surface potential Ψ_0 (in V) (Fig. 5).

In the field generated by the complexed cations, solvated anions are attracted and form a double layer. The distance of 5 Å represents approximately the closest approach of the solvated anions. The other counter ions are distributed following a Boltzmann distribution and form the diffuse layer whose

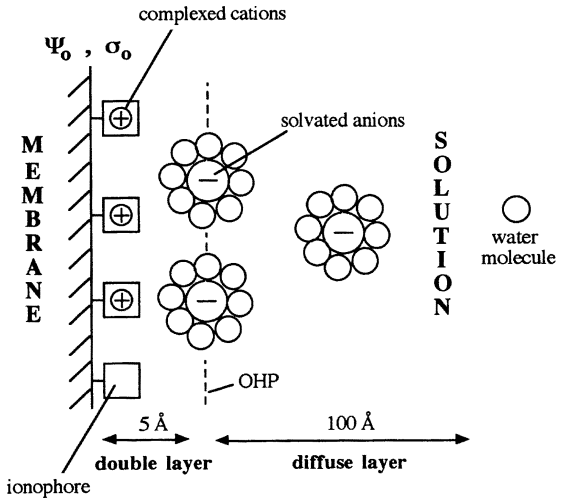

Fig. 5 Schematic representation of the membrane/analyte interface following the site binding model. σ_0 is the excess positive charge density (C cm^{-2}), Ψ_0 is the corresponding potential (V) and OHP is the outer Helmholtz plane. From ref. 12 with permission of the publisher

thickness depends on the ionic strength. A value of 100 Å is expected for electrolyte concentrations of the order of 10^{-3} M in water.[22]

The chemical equilibria arising at the membrane/analyte interface are:

$$M^+ \rightleftharpoons M_s^+ \quad (1)$$

$$L_s + M_s^+ \rightleftharpoons L_sM_s^+ \quad (2)$$

with M^+, M_s^+ being the cation concentration (in M) in the bulk solution and in the double layer, respectively; L_s denotes the free binding sites and $L_sM_s^+$ the complexed surface sites (in molecules per cm^2). The total density of sites, N_{TOT}, is given by:

$$N_{TOT} = [L_sM_s^+] + [L_s] \quad (3)$$

The silica surfaces are usually pH sensitive and proton binding sites L_s' should normally also be considered.[20] However, all present experiments have been carried out in buffer solutions.

An ionophore–ligand stability constant may be defined within the double layer, at the grid/analyte interface:

$$K' = [L_sM_s^+]/[L_s][M_s^+] \quad (4a)$$

$$K = K'/[\text{solvent}] \quad (4b)$$

It is noteworthy that the constant thus defined differs from the one effective in the bulk solution. The concentration of cation M_s^+ is related to the bulk concentration *via* a Boltzmann distribution to take into account the repulsive forces induced by the complexed interfacial cations:

$$[M_s^+] = [M^+]\exp(-q\Psi_0/k_BT) \quad (5)$$

where Ψ_0 is the potential corresponding to the excess interfacial positive charges, q is the charge and k_B is Boltzmann's constant. This expression is valid whenever monovalent cations are considered.

It can be then postulated that the conventional capacitance law applies:

$$\sigma_0 = C_{dl}\Psi_0 \quad (6)$$

where σ_0 is the number of charges per cm^2, C_{dl} is the double layer capacitance and Ψ_0 is the surface potential.

The double layer capacitance has been shown experimentally to vary only slightly with the nature of the electrolyte and the ionic strength. A value of 20 μF cm^{-2} is generally taken[20,23] and it is considered to be constant.

From previous equations, it can be readily demonstrated that:

$$[M^+] = \frac{[L_sM_s^+]}{K[L_s]\exp(-q\Psi_0/k_BT)} \quad (7)$$

since

$$q[L_sM_s^+] = \sigma_0 = C_{dl}\Psi_0 \quad (8)$$

In the case that the cation L_s and proton L_s' binding sites are considered as independent, the last equation should be written as:

$$q[L_sM_s^+] + q[L_s'H^+] = \sigma_0 = C_{dl}\Psi_0 \quad (9)$$

In this case, differential measurements between grafted and ungrafted devices should be carried out.[21] However, these two different devices have different pH dependences. The model described in ref. 21 thus cannot be used rigorously but the numbers derived from it can be considered as good approximations (see below).

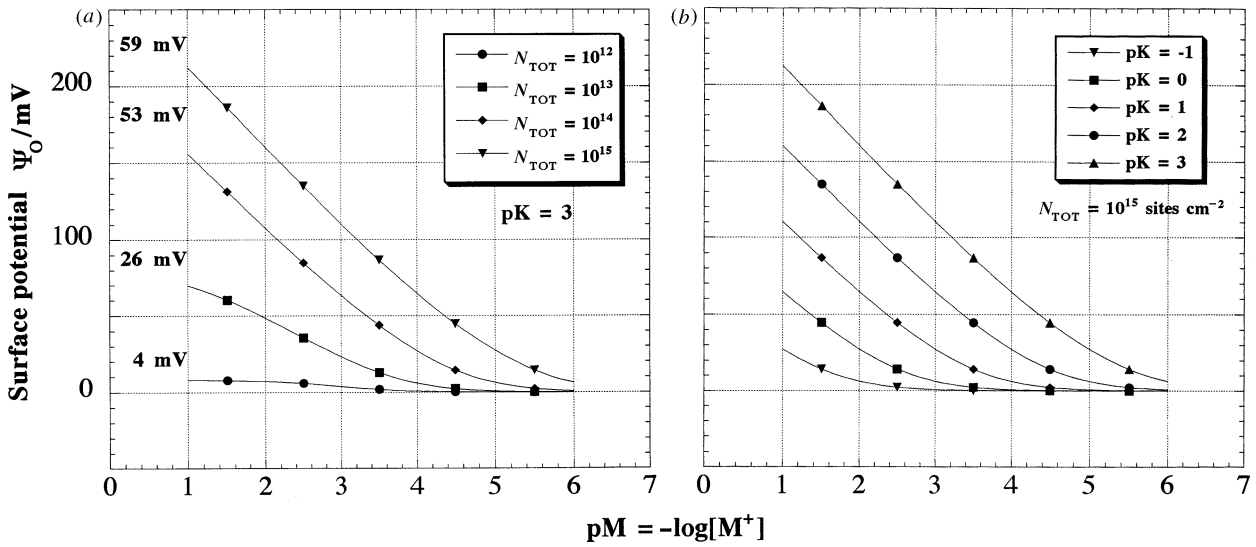

Fig. 6 Theoretical surface potential (Ψ_0) as a function of the logarithm of the cation concentration (pM = $-\log[M^+]$). (*a*) For different values of the binding site density, N_{TOT} (at $K = 10^3$). The slope corresponding to the different curves is indicated. (*b*) For different values of the cation–ligand association constant, log K = pK (at $N_{TOT} = 10^{15}$ sites cm^{-2}) (modified from ref. 12)

$$N_{TOT} = \frac{C_{dl}\Psi_0}{q} + [L_s] \quad (10)$$

$$\frac{[L_s]}{[L_sM_s^+]} = \frac{qN_{TOT}}{C_{dl}\Psi_0} - 1 \quad (11)$$

$$-\log[M^+] = \log K + \log\left(\frac{qN_{TOT}}{C_{dl}\Psi_0} - 1\right) - \frac{1}{\ln 10}\frac{q\Psi_0}{k_BT} \quad (12)$$

The previous model only takes into account surface binding sites whereas the membrane presently used is, on the average, 200 Å thick. A distribution of ions within the grid membrane should be considered. However, the previous simple modelling will enable us to fit the experimental titration curves satisfactorily as a function of the two main parameters: N_{TOT}, the total density of binding sites and K, the cation–ligand association constant (Fig. 6).

The model predicts that a density of surface binding sites of the order of 10^{14}–10^{15} sites per cm^2 is necessary to have a slope around the Nernstian value (59 mV). On the other hand, an increase of the ionophore–ligand stability constant leads to a decrease of the ion detection threshold. The values of N_{TOT} and K will be calculated from the experimental curves by fitting them with the theoretical ones.

Remarkable points in the $-\log[M^+]$ *vs.* Ψ_0 equation corresponding to:

$$[L_s] = [L_sM_s^+] = \tfrac{1}{2}N_{TOT} \quad (13)$$

can be considered. From previous equations it may be readily demonstrated that, with the previous condition, the slope of the curves at this point is given by:

$$\left[\frac{d\Psi_0}{d(pM)}\right]_{\frac{1}{2}} = -\frac{\ln 10}{\frac{q}{k_BT} + \frac{4C_{dl}}{qN_{TOT}}} \quad (14)$$

With $pM = -\log[M^+]$:

$$(\Psi_0)_{\frac{1}{2}} = \frac{qN_{TOT}}{2C_{dl}} \quad (15)$$

$$(pM)_{\frac{1}{2}} = \log K - \frac{1}{\ln 10}\frac{q^2N_{TOT}}{2C_{dl}k_BT} \quad (16)$$

Simple calculations show that for $N_{TOT} = 10^{15}$ per cm^2, saturation of the surface binding sites is not possible since $(pM)_{\frac{1}{2}} = -64$; for $N_{TOT} = 10^{13}$ such a saturation can be reached for $(pM)_{\frac{1}{2}} = 2.3$.

The $[d\Psi_0/d(pM)]_{\frac{1}{2}}$ term depends only on N_{TOT}, whereas $(pM)_{\frac{1}{2}}$ is related to both K and N_{TOT}.

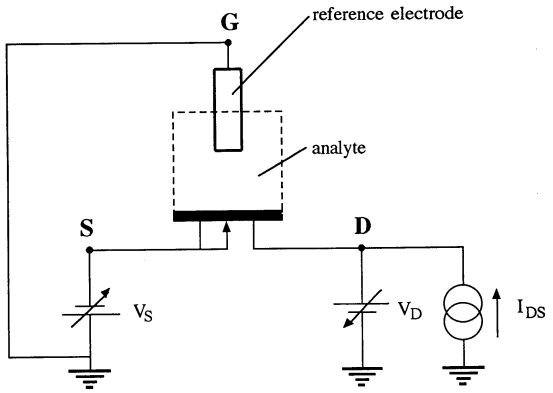

Fig. 7 Electrical circuit for studying ISFET devices. S: source; D: drain; I_{DS} and V_{SD} are maintained constant

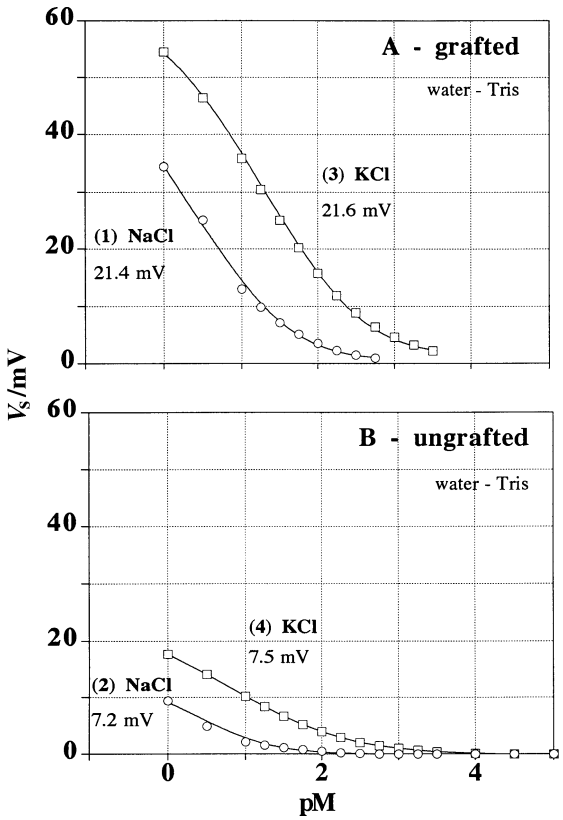

Fig. 8 Variation of V_S as a function of the concentration of NaCl and KCl in water [tris(hydroxymethyl)aminomethane–HCl: 10^{-1} M; pH = 6.7)]. Experiments 1–4 (see Table 1)

Table 1 ISFET response (V_S) in water [buffer: 10^{-1} M tris(hydroxymethyl)aminomethane–HCl, pH = 6.7] as a function of the Na^+ or K^+ concentrations

Expt	Configuration[a]	Salt	Exptal $(slope)_{\frac{1}{2}}$/mV	Fitted $(slope)_{\frac{1}{2}}$/mV	Calcd N_{TOT} × 10^{12}/cm^{-2}	Calcd pK
1	A	NaCl	21.4	20.5	7.0	0.8
2	B	NaCl	7.2	6.8	1.7	0.5
3	A	KCl	21.6	21.9	7.5	1.8
4	B	KCl	7.5	9	2.3	1.6
5	A–B	NaCl	12.8	13.0	3.6	1.1
6	A–B	KCl	16.4	17.2	5.2	1.8

[a] A: surface grafted with substituted phthalocyanine and methacrylate; B: surface grafted only with (trimethoxysilyl)propyl methacrylate (in both cases an ECS reference is used and single measurements are made); A–B: differential measurements of the A and B ISFETs (Pt reference electrode). $(Slope)_{\frac{1}{2}} = -[d\Psi_0/d(pM)]_{\frac{1}{2}}$.

Table 2 ISFET response in MeOH–H_2O (90 : 10; v : v) as a function of the Na^+ or K^+ concentrations (buffer: 10^{-1} M lithium succinate, pH = 6.3, see ref. 24)

Expt	Configuration[a]	Salt	Exptal $(slope)_{\frac{1}{2}}$/mV	Fitted $(slope)_{\frac{1}{2}}$/mV	Calcd $N_{TOT} \times 10^{12}/cm^{-2}$	Calcd pK
7	A	NaSCN	38	39	24	1.5
8	B	NaSCN	21.6	19.1	6.1	1.5
9	A	KSCN	38	36.5	20	2.9
10	B	KSCN	33.8	31.1	14	1.8
11	A–B	NaSCN	15	15.1	4.4	2.0
12	A–B	KSCN	14.5	14.5	4.1	3.2

[a] Same legend as Table 1.

Experimental results. The electrical circuit used to study the fabricated ISFET is shown in Fig. 7. The response to the measurements have been carried out in such a way that the source-to-drain current I_{DS} and the source-to-drain voltage V_{DS} remain constant; for that V_S is varied. In our case, V_{DS} = 0.5 V, and I_{DS} = 100 μA. The V_S voltage is measured against a reference electrode ($V_S = -V_{GS}$).

The main parameters involved in the grid-to-source voltage V_{GS} are:

$$V_{GS} = \Psi_{SiO_2} - \Psi_0 + V_{ref} + V_{el} + V_{dif} + \cdots \quad (17)$$

Ψ_{SiO_2} is the potential across the grid dielectric. When a salt is added to the solution, V_{ref} (electrode potential), V_{el} (ohmic drop in the electrolyte) and V_{dif} (potential of the diffuse layer) are considered to remain constant whereas Ψ_0 and V_{GS} vary.

Two different ISFETs have been tested. In the first one the grid membrane is made of the photopolymerized phthalocyanine derivative (type A, grafted); in the second one, the silica surface of the grid has been treated only with (trimethoxysilyl)propyl methacrylate (type B, ungrafted).

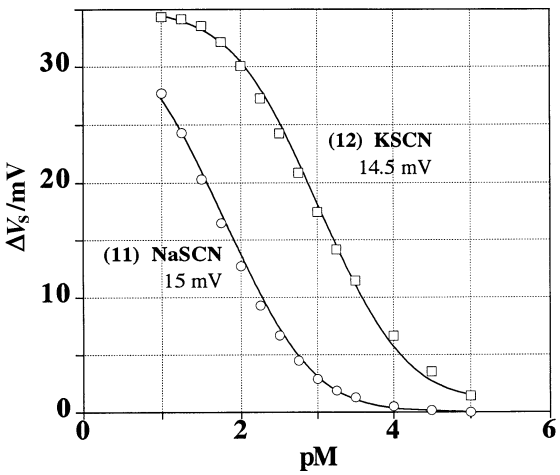

Fig. 9 Differential measurements (A–B type) for the ISFET in the presence of various concentrations of NaSCN and KSCN. (Experiments 11 and 12). Solvent: MeOH–H_2O (90 : 10; v : v); buffer: 10^{-1} M lithium succinate, pH = 6.3; reference: platinum electrode

Measurements have been first carried out in water in the presence of a tris(hydroxymethyl)aminomethane–HCl buffer, tris–HCl (10^{-1} M, pH = 6.7) (Table 1). Single ISFET measurements (A or B) demonstrate that the slope of the curve, and correspondingly the total number of surface states, is higher for the amphiphilic Pc-containing membrane than for the methacrylate-functionalized surface. It is also apparent that K^+ ion leads to lower threshold ion detections (and a higher ligand–ion stability constant) than Na^+ (Fig. 8) for both phthalocyanine and phthalocyanine-free membranes. However, as previously outlined, it is better to consider differential measurements. These latter (noted A–B) allowed us to characterize the A-type ISFET against the B-type one. In this configuration, the maximum slope of the V_S *vs.* $-\log[M^+]$ plots is reduced to 12–16 mV and both the total number of binding sites and the cation–ligand association constant seem to be of the same order of magnitude for Na^+ and for K^+.

It is well-known that the cation–ligand association constants are larger in methanol–water mixtures than in pure water. For this reason, the experiments have been repeated in MeOH–H_2O (90 : 10, v : v) at pH = 6.3 (10^{-1} M lithium succinate buffer[24]) (Table 2).

For differential measurements, contrary to the determinations in water, the ion detection threshold is significantly different between Na^+ and K^+, whereas the effective density of sites (and therefore the corresponding slopes) are approximately equal (Fig. 9). The density of binding sites is around 4×10^{12} in water, as in MeOH–H_2O, whereas, as expected, the apparent association constant (K) is larger by more than one order of magnitude in MeOH–H_2O than in pure water.

However, most of the practical applications of ISFET concern aqueous media and therefore the chemical mechanisms arising in water have been more thoroughly studied. The effect of the tris–HCl buffer concentration on the ISFET characteristics was studied and surprising results were found (Table 3). In the absence of buffer $-[d\Psi_0/d(pM)]_{\frac{1}{2}}$ is *negative* for the phthalocyanine-containing membrane (A). These

Table 3 Effect of the concentration of buffer [tris(hydroxymethyl)aminomethane–HCl, pH = 6.7] on the ISFET characteristics (individual measurements). Solvent: water

Expt	Configuration[a]	Salt	Medium	Exptal $(slope)_{\frac{1}{2}}$/mV
13	A	NaCl	H_2O	−10
14	A	NaCl	10^{-2} M Tris	−4
1	A	NaCl	10^{-1} M Tris	21.4
15	A	KCl	H_2O	−30
16	A	KCl	10^{-2} M Tris	−4
3	A	KCl	10^{-1} M Tris	21.6

[a] Same legend as Table 1.

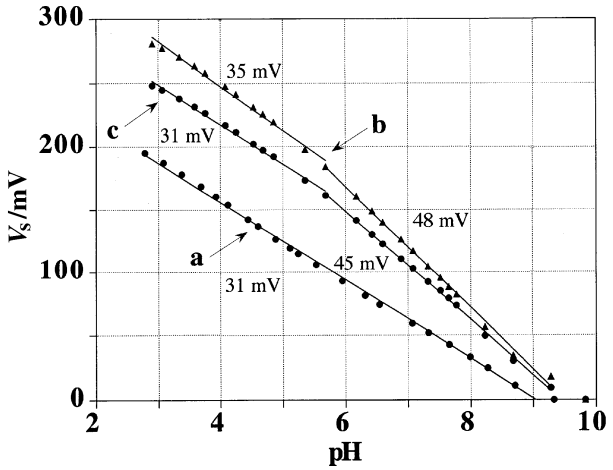

Fig. 10 Variation of V_S as a function of the HCl concentration. Solvent: H_2O; buffer: 10^{-2} M tris(hydroxymethyl)aminomethane; reference: calomel electrode. (curve a) Phthalocyanine-containing membrane (A-type); (curve b) methacrylate-functionalized surface (B-type); (curve c) virgin SiO_2 surface

results are observed for both NaCl and KCl. At higher concentrations of buffer, a positive sign is observed. This indicates that *anions* are incorporated within the Pc-containing membrane whenever the Cl^- concentration in the buffer is not sufficient relative to the added electrolyte to saturate the anionic sites. The nature of these binding sites is discussed later on. At high buffer concentrations (10^{-1} M), the anionic binding sites are saturated and the addition of potassium or sodium chloride does not alter significantly the overall anion concentration in the membrane. This also means that the ammonium salt of the buffer is far less complexed than Na^+ and K^+. For a buffer concentration of 10^{-2} M, it seems that the anion (Cl^-) and the cation (Na^+ or K^+) correspond to the same density of sites, leading to $[d\Psi_0/d(pM)]_{\frac{1}{2}} = 0$.

The pH dependence of the ISFET has also been studied (Fig. 10). The concentration of tris–HCl buffer used (10^{-2} M) is not sufficient to saturate the anionic binding sites but in the range of pH studied (2–9) this does not influence the curves. For the three cases studied: (*i*) phthalocyanine-containing membrane (A-type), (*ii*) methacrylate-functionalized surface (B-type) and (*iii*) virgin SiO_2 surface, a very important pH dependence is found. In all cases, two domains of pH may be defined: 3–5 (slope: 30–35 mV) and 6–9 (slope: 45–50 mV). The functionalization of SiO_2 with (trimethoxysilyl)propyl methacrylate gives a slightly higher number of binding sites: the slope is 35 mV instead of 31 mV for the virgin SiO_2 layer (pH range 3–5). The use of the phthalocyanine-containing membrane decreases significantly the pH sensitivity of the device (slope: 31 mV, pH range: 6–9).

A more precise insight into the chemical nature of the binding sites may be gained from what is already known of the acidity constant of interfacial silanol groups:[25]

$$H_2O + \equiv SiOH \overset{K_1}{\rightleftharpoons} \equiv SiO^- + H_3O^+ \quad K_1 = 4 \times 10^{-6}$$

$$H_2O + \equiv SiOH_2^+ \overset{K_2}{\rightleftharpoons} \equiv SiOH + H_3O^+ \quad K_2 = 10$$

Both anionic ($\equiv SiO^-$) and cationic ($\equiv SiOH_2^+$) sites are present at the interface; their relative abundance is correlated to the pH of the bulk solution. For an acid-treated SiO_2 surface:[26]

$$N_{TOT} = [\equiv SiOH] + [\equiv SiO^-] + [\equiv SiOH_2^+]$$
$$= 5 \times 10^{15} \text{ sites cm}^{-2}$$

From the values of K_1 and K_2 it can be readily calculated that at pH = 6.7: $[\equiv SiOH] = 4.8 \times 10^{14}$ sites cm^{-2}, $[\equiv SiO^-] = 2 \times 10^{13}$ sites cm^{-2} and $[\equiv SiOH_2^+] = 4 \times 10^9$ sites cm^{-2}

When a salt MX is added to the solution, both anionic and cationic binding can occur:[23]

$$\equiv SiO^- + M^+ \rightleftharpoons \equiv SiO^-, M^+$$

$$\equiv SiOH_2^+ + X^- \rightleftharpoons \equiv SiOH_2^+, X^-$$

The proton forms more stable ion pairs with the silanolate moiety ($K_1 = 4 \times 10^{-6}$) than Na^+ or K^+; the difference is approximately five orders of magnitude (Table 1).

At low tris–HCl concentrations, the formation of ion pairs with the $\equiv SiOH_2^+$ sites is affected by the concentration of the electrolyte (NaCl or KCl) added and anion complexation may be detected.

Conclusion

In conclusion, two new phthalocyanine derivatives, **1a** and **1b** substituted with polyoxyethylene sidechains that are substituted with hydroxy or methacrylate groups, have been synthesized. The first derivative has been shown to form mesophases by various physicochemical characterization methods; the second one has been photocopolymerized at the silica surface of an ISFET grid previously treated with (trimethoxysilyl)propyl methacrylate. The detection of ions (H^+, Na^+, K^+, Cl^-) is possible with such a device. It has been demonstrated that both the amphiphilic Pc polymer and the various silanol sites ($\equiv SiO^-$, $\equiv SiOH$, $\equiv SiOH_2^+$) are important for determining the ion response of the ISFET. The various chemical equilibria arising at the SiO_2–membrane–analyte interfaces as well as the most plausible structure of the molecular-material-based membrane are schematically summarized in Fig. 11.

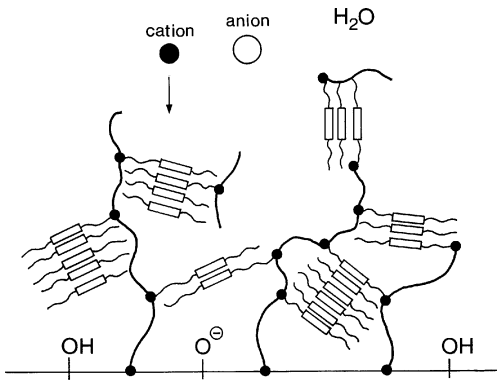

Fig. 11 Schematic representation of the SiO_2–membrane–analyte interfaces

Experimental

The compounds were characterized by IR, UV/VIS, mass and nuclear magnetic resonance spectroscopies. IR spectra were recorded on a Perkin-Elmer FTIR spectrometer. UV/VIS absorption spectra were measured with a Kontron UVIKON 360 spectrophotometer. FAB and MALDI-TOF mass spectrometry measurements were carried out at the 'Servicio Interdepartamental de Investigacion (SIdI)' at the Universidad Autonoma de Madrid and at the 'Service de spectrométrie de masse' at Jussieu (Paris), respectively. NMR spectra were recorded with a Bruker AM 300 spectrometer.

The microelectronics circuits used have been fabricated at the 'Centre Interuniversitaire de Microélectronique' (Grenoble), and the ISFET has been realized in a clean room at ESIEE (Noisy le Grand).

Syntheses

All chemicals and solvents were reagent grade and were employed without further purification. 4,5-Dibromocatechol **2** was prepared by reacting pyrocatechol with molecular bromine in carbon tetrachloride.[13] 1-Chloro-8-methoxy-3,6-dioxaoctane was synthesized from triethylene glycol monomethyl ether according to a procedure previously reported.[27,28]

4,5-Dibromo-1-hydroxy-2-(1′,4′,7′,10′-tetraoxaundecyl)benzene (3). To a solution of 10.7 g (40 mmol) of dibromocatechol in 100 ml of butanol was added 3.8 g of NaOH dissolved in 20 ml of water; argon gas was then bubbled through the solution for 15 min. The mixture was then heated under reflux and 11 g (60 mmol) of 1-chloro-8-methoxy-3,6-dioxaoctane was added dropwise with stirring. When the addition was completed, the reaction mixture was heated at reflux under argon for 16 h. After cooling, 1 ml of concentrated HCl was added and the crude mixture was filtered, concentrated under vacuum, and extracted with CH_2Cl_2 (3 × 200 ml). The crude oil obtained was purified by chromatography on silica gel (eluent, CH_2Cl_2–Et_2O, 50 : 50), yielding 6.08 g of a yellow oil (41%). ^{1}H NMR ($CDCl_3$, 300 MHz): δ 3.38 (s, 3H, OCH_3), 3.6–3.8 (m, 8H, CH_2O), 3.82 (t, 2H, J = 4.6 Hz, $PhOCH_2CH_2$), 4.12 (t, 2H, J = 4.6 Hz, $PhOCH_2$), 7.10 (s, 1H, ArH), 7.18 (s, 1H, ArH). ^{13}C NMR ($CDCl_3$, 75 MHz): δ 58.8, 69.1, 70.2, 70.3, 70.4, 71.2, 71.7, 112.8, 116.8, 119.3, 120.4, 144.8, 146.0. FAB-MS (*m*-NBA): *m*/*z* 413 ($M^+ + 1$), 436 ($M^+ + Na$). (The assignment is given as an indication; calibration errors may occur). CI-MS (NH_3): *m*/*z* 430, 432, 434 [($M^+ + 1 + NH_3$), with a dominant contribution from the Br isotopes], 413, 415, 417 ($M^+ + 1$).

1,2-Dicyano-3-hydroxy-4-(1′,4′,7′,10′-tetraoxaundecyl)benzene (4). A mixture of 5.07 g (12.2 mmol) of **3**, 3.3 g (37 mmol) of CuCN and 100 ml of freshly distilled DMF was refluxed under argon for 16 h. After being cooled, the reaction mixture was poured into 1 l of a solution of 6 g (37 mmol) of $FeCl_3$ in 5% aqueous HCl and heated to 80 °C under stirring. This solution was then extracted with ethyl acetate and the organic layer was washed with 5% aqueous HCl and distilled water, and dried finally over $MgSO_4$. The resulting orange oil was purified by chromatography on alumina Brockman 5 (eluent, CH_2Cl_2–MeOH, 98 : 2) to give 1.3 g (36%) of **4** as a yellow oil. ^{1}H NMR ($CDCl_3$, 300 MHz): δ 3.40 (s, 3H, OCH_3), 3.5–3.8 (m, 8H, CH_2O), 3.92 (t, 2H, J = 4.6 Hz, $PhOCH_2CH_2$), 4.25 (t, 2H, J = 4.6 Hz, $PhOCH_2$), 7.16 (s, 1H, ArH), 7.23 (s, 1H, ArH). ^{13}C NMR ($CDCl_3$, 75 MHz): δ 58.7, 68.6, 68.7, 69.9, 70.0, 70.5, 71.7, 106.5, 109.8, 116.9, 120.6, 149.8, 151.7. FAB-MS (*m*-NBA): *m*/*z* 307 ($M^+ + 1$), 328 ($M^+ + Na$). CI-MS (NH_3): *m*/*z* 324 ($M^+ + 1 + NH_3$), 307 ($M^+ + 1$). An impurity at 333 is detected corresponding to the displacement of OH by the NMe_2 group.

1,2-Dicyano-4-(9′-hydroxy-1′,4′,7′-trioxanonyl)-2-(1′,4′,7′,10′-tetraoxaundecyl)benzene (5). A mixture of 1.1 g (3.6 mmol) of **4**, 845 mg (5 mmol) of 1-chloro-8-hydroxy-3,6-dioxaoctane, 970 mg (7 mmol) of K_2CO_3 and 30 ml of DMSO was stirred at 100 °C under argon for 3 days. After cooling, the solvent was evaporated under reduced pressure. CH_2Cl_2 and water (200 ml each) were then added to the crude mixture, and the aqueous layer was extracted (3 × 200 ml) with CH_2Cl_2. The combined organic extracts were washed with 5% aqueous $NaHCO_3$ and water (3 × 200 ml) and dried over $MgSO_4$ to yield 1.1 g (70%) of **5** as a yellow oil. ^{1}H NMR ($CDCl_3$, 300 MHz): δ 3.32 (s, 3H, OCH_3), 3.4–3.9 (m, 16H, CH_2O), 3.86 (t, 4H, J = 4.6 Hz, $PhOCH_2CH_2$), 4.20 (t, 4H, J = 4.6 Hz, $PhOCH_2$), 7.22 (s, 2H, ArH). ^{13}C NMR ($CDCl_3$, 75 MHz): δ 58.8, 61.4, 69.2, 70.4, 70.5, 70.8, 71.7, 72.4, 108.5, 108.6, 115.6, 115.7, 116.8, 116.9, 152.1, 152.2. FAB-MS (*m*-NBA): *m*/*z* 439 ($M^+ + 1$), 461 ($M^+ + Na$). CI-MS (NH_3): *m*/*z* 456 ($M^+ + 1 + NH_3$), 439 ($M^+ + 1$). A small amount (15%) of an adduct of triethylene glycol is detected at 589 (ionization: CH_4).

[2,9,16,23-Tetrakis(9′-hydroxy-1′,4′,7′-trioxanonyl)-3,10,17,24-tetrakis(1′,4′,7′,10′-tetraoxaundecyl)]phthalocyaninato zinc(II) (1a) (mixture of isomers). Phthalonitrile (440 mg, 1 mmol), 5.48 mg (0.35 mmol) of $ZnCl_2$, 114 mg (0.75 mmol) of DBU and 3 ml of hexanol were degassed with argon and heated under reflux under an inert atmosphere overnight. After cooling, the reaction mixture was extracted with water and Et_2O to eliminate the hexanol. The green product was extracted from the aqueous layer with dichloromethane–ethanol (1 : 1) and washed several times with distilled water. The crude product was purified by preparative thin layer chromatography [neutral alumina, 2 mm thickness; eluent CH_2Cl_2–MeOH, 96 : 4 (v : v); R_f = 0.15]. A final purification was achieved by recrystallization from a mixture of CH_2Cl_2–hexane (1 : 1, v : v) to afford 116 mg (26%) of a dark green paste. Anal. calcd. (%) for $C_{84}H_{120}N_8O_{32}Zn$ (MW = 1816): C, 55.51; H, 6.61; N, 6.17. Found: C, 55.09; H, 6.52; N, 6.00. ^{1}H NMR ([$^2H_6$]DMF, 300 MHz): δ 3.37 (s, 12H, OCH_3), 3.5–4.0 (m, 64H, CH_2O), 4.18 (m, 16H, J = 4.6 Hz, $PhOCH_2CH_2$), 4.77 (m, 16H, J = 4.6 Hz, $PhOCH_2$), 9.1 (br, 8H, ArH). MALDI-TOF-MS *m*/*z* 1819 ($M^+ + 3$). UV/VIS ($CHCl_3$): λ_{max}/nm (log ε) 676 (5.42), 631 (sh), 610 (4.77), 355 (5.15).

[2,9,13,23-Tetrakis(9′-methacryloxy-1′,4′,7′-trioxanonyl)-3,10,17,24-tetrakis(1′,4′,7′,10′-tetraoxaundecyl)]phthalocyaninato zinc(II) (1b) (mixture of isomers). To a solution of 31 mg (17.07 μmol) of phthalocyanine derivative **1a**, and 71.2 μl (51.7 mg, 0.5 mmol) of triethylamine in 2 ml of dry CH_2Cl_2 stabilised with amylene was added 33.4 μl (35.7 mg, 0.34 mmol) of methacryloyl chloride; the mixture was kept under argon overnight at room temperature. The reaction mixture was diluted with chloroform and the organic solution was washed with 10% aqueous $NaHCO_3$, rinsed with distilled water, and dried over $MgSO_4$, filtered, and concentrated under vacuum. A final purification was achieved by column chromatography over preparative thin layer chromatography [neutral alumina, 2 mm thickness; eluent $CHCl_3$–AcOEt–EtOH, 60 : 36 : 4 (v : v : v); R_f = 0.25], yielding 15 mg (42%) of a dark green product. MALDI-MS: *m*/*z* 2089 ($M^+ + 1$).

Treatment and functionalization of the grid

A solution of sulfochromic acid (1 ml saturated aqueous $K_2Cr_2O_7$, 19 ml concentrated H_2SO_4) was used to treat the silica surface of the grid for 3 min. It was rinsed and left in ultrapure water for 18 h, and dried in a stream of nitrogen.

The functionalization with 3-(trimethoxysilyl)propyl methacrylate has been previously described.[12] The methacrylate-functionalized phthalocyanine **1b** was then copolymerized under irradiation onto the grid silica grafted with the trimethoxysilane derivative. 2,2′-Dimethoxyphenylacetophenone (Janssen) was used as the photoinitiator. A solution constituted of **1b** (0.3%, w : w) and the photoinitiator (0.012%, w : w) in chloroform was spin-coated onto the surface of the grid (1500 rpm, 20 s). The coated layer was then exposed to ultraviolet light (mercury lamp, 364 nm) under nitrogen for 10 min. Irradiation was carried out through a mask in order to obtain the polymerized film at the desired position.[12] The non-exposed parts were removed with toluene.

Atomic force microscopy (AFM). An optical beam AFM (deflection type) was used in the contact mode (Nanoscope II, Digital Instruments). The sensor was a standard microfabricated V-shaped cantilever. The experiments were performed in air under ambient conditions.

The sample described in this study was prepared from a silicon (100) wafer onto which a thin layer of polymerized phthalocyanine **1b** was synthesized.

Thickness measurements by ellipsometry. Measurements have been carried out on two different apparatus at the Collège de France (L. Léger) and the ESPCI. For reasons of brevity only the latter ones are described below in detail. A commercial SOPRA ES 4G spectroscopic ellipsometer was used. The optical system was constituted by a rotating polarizer, the sample and an analyzer. The diameter of the focused beam spot was 150 μm. The angle of incidence relative to the normal of the plane of the sample was 75°. All samples were derived from silicon (100) wafers. The ellipsometric parameters cos Δ and tan Ψ were recorded as a function of the wavelength. Δ is the phase difference and tan Ψ the amplitude ratio of the complex reflection coefficients of the electrical field components parallel and perpendicular to the plane of incidence. The film thickness and the refractive index calculations were carried out from ellipsometric parameters using standard optical models. The thickness of the functionalized layer (SiO_2 treated with the trimethoxysilane derivative) was determined by comparison with a naked substrate. Thickness values were obtained by using six different wavelengths in the range 0.45–0.50 μm. We assumed in the case of the methacrylate-functionalized substrate that the SiO_2-functionalized layer was equivalent to unmodified silica with a refractive index of 1.46.

The sample fabricated for AFM study was used to determine the complex refractive index, n–ik, and the thickness of the polymerized phthalocyanine thin layer. Ellipsometric parameters were measured from 0.26 to 0.85 μm (237 points). The thickness of the layer was evaluated in the quasi-transparent domain from 0.78 to 0.82 μm. We found a thickness of about 355 Å. In this calculation, a bilayer structure was postulated. The first layer is made up of the trimethoxysilane derivative reacted with the silica surface and the SiO_2 layer itself (thickness around 20 Å, natural oxidation of silicon). The second layer is constituted of the polymerized phthalocyanine-based membrane.

The values of the real and the imaginary parts of the complex index were then calculated in the range from 0.26 to 0.85 μm. At 500 nm, far from the absorption band, the refractive index n is 1.56. The coefficient k was 0.27 at 630 nm, corresponding to the absorption of the phthalocyanine chromophore. In the UV domain, the maxima are at 290 and 345 nm ($k = 0.16$ and 0.20 respectively).

When the membrane is covalently linked to the surface, transformations of the UV/VIS and ellipsometric characteristics have been noticed. In air and under UV irradiation, rapid conversion (in a few hours) occurs. Some modifications are also noticed by heating at 70 °C for 20 h. The layers used for ISFET measurements are not expected to have undergone significant changes as compared to the initial ones, since they were kept in the dark and no transformation was noticed during the measurements, which lasted approximately three weeks (room temperature). In all cases, the devices show reversible characteristics with a shift on the order of 1 mV per hour for ion titration. A more exhaustive study of these points will be published in the near future.[29]

ISFET measurements. The ISFET devices were studied with an amplifier system (Microspecials) at constant drain current I_{DS} and constant source-to-drain voltage V_{DS} (see Fig. 7). I_{DS} was equal to 100 μA and V_{DS} equal to 0.5 V. V_S was plotted with a recorder (Linseis). A standard reference calomel electrode has been used for the titrations in water. LiCl (1 M) in MeOH–H_2O (90 : 10; v : v) has been used to fill the reference calomel electrode in the case of the titrations in this solvent mixture. pH Variations were controlled with a digital pHmeter (Tacussel MINI-80) by addition of 1 M HCl in the starting solution containing 121 mg of tris(hydroxymethyl)aminomethane (Prolabo rectapur) in 100 ml of distilled water. Ion titrations was made with 1 M solutions of the salt in 100 ml of buffer solution. NaCl, KCl, LiOH and succinic acid were purchased from Prolabo, NaSCN and KSCN from Aldrich.

In water the fit calculations were carried out in the concentration range of $1–10^{-5}$ M and in the interval $10^{-1}–10^{-5}$ M in MeOH–H_2O (90 : 10).

ISFET encapsulation. The final devices were obtained by depositing a protective layer to avoid short circuits between the connection wires of the source, the drain and the analyte. This has been carried out using an epoxy resin (Epotecny E 708), which was deposited manually.

Transmission electron microscopy. The layers were peeled from the substrate using a 0.1 M KOH solution and put on a microscope grid. Images and electron diffraction patterns were realized with a JEOL 100CX transmission electron microscope.

Optical microscopy and DSC. The textures and the phase transitions have been observed with a Leitz Orthoplan microscope equipped with a Mettler F82 hot stage. Differential scanning calorimetry experiments have been carried out on a Perkin-Elmer DSC-4 equipped with a 3600 data station.

X-Ray measurements. The X-ray measurements were carried out using CuKα radiation (a flat graphite crystal was used as monochromator). The X-ray powder diagrams were recorded on flat films. The samples were contained in 1 mm diameter Lindemann glass tubes. The sealed capillary tubes were mounted in an electrically heated oven. The temperature was controlled within ±0.1 °C using a platinum resistor. X-Ray experiments were carried out under reduced pressure.

Acknowledgements

This research was financially supported by EC grant 940558, by the city of Paris and by the CNRS. J. C. Tabet (Université P. & M. Curie) and N. Morin (ENS) are thanked for the MALDI-TOF and CI experiments, respectively. C. Chassagnard and C. Jallabert (ESPCI-CNRS) is thanked for the NMR studies. A. Maillard (ESIEE) is gratefully acknowledged for his assistance. L. Léger (Collège de France) is thanked for her help during ellipsometric measurements.

References

1 P. Bergveld, *IEEE Trans. Biomed. Eng.*, BME 1970, **17**, 70.
2 P. Clechet, *Sensors Actuators B*, 1991, **4**, 53.
3 J. Janata, *Chem. Rev.*, 1990, **90**, 691.
4 Z. Brzozka, P. L. H. M. Cobben, D. N. Reinhoudt, J. J. H. Edam, J. Buter and R. M. Kellog, *Anal. Chim. Acta*, 1993, **273**, 139.
5 C. Piechocki, J. Simon, A. Skoulios, D. Guillon and P. Weber, *J. Am. Chem. Soc.*, 1982, **104**, 5119.
6 D. Guillon, P. Weber, A. Skoulios, C. Piechocki and J. Simon, *J. Mol. Cryst. Liq. Cryst.*, 1985, **130**, 223.
7 C. Piechocki and J. Simon, *Nouv. J. Chim.*, 1985, **3**, 159.
8 J. Vacus and J. Simon, *Adv. Mater.*, 1995, **7**, 797.
9 M. Armand, *Ann. Rev. Mater. Sci.*, 1986, **16**, 245.
10 M. A. Ratner and D. F. Schriver, *Chem. Rev.*, 1988, **88**, 109.
11 T. Toupance, P. Bassoul, L. Mineau and J. Simon, *J. Phys. Chem.*, 1996, **100**, 11704.
12 T. Thami, J. Simon, N. Jaffrezic, A. Maillard and S. Spirkovitch, *Bull. Soc. Chim. Fr*, 1996, **133**, 759.

13 C. F. Van Nostrum, S. J. Picken, A-J. Schouten and R. J. M. Nolte, *J. Am. Chem. Soc.*, 1995, **117**, 9957.
14 For an example see: M. S. Newman, *Org. Synth.*, 1962, **95**, 2098.
15 D. Lelièvre, L. Bosio, J. Simon, J.-J. André and F. Bensebaa, *J. Am. Chem. Soc.*, 1992, **114**, 4475.
16 V. Rocher, J. M. Chovelon, N. Jaffrezic-Renault, Y. Cros and D. Birot, *J. Electrochem. Soc.*, 1994, **141**, 535.
17 J. M. Chovelon, J. J. Fombon, P. Cléchet, N. Jaffrezic-Renault, C. Martelet and A. Nyamsi, *Sensors Actuators B*, 1992, **8**, 221.
18 J. Vacus, P. Doppelt, J. Simon and G. Memetzidis, *J. Mater. Chem.*, 1992, **2**, 1065.
19 P. G. De Gennes, *J. Phys. Lett.*, 1983, **44**, L657.
20 H. Perrot, N. Jaffrezic-Renault and P. Cléchet, *J. Electrochem. Soc.*, 1990, **137**, 598.
21 H. Perrot, N. Jaffrezic-Renault, N. F. Rooij and H. van den Vlekkert, *Sensors Actuators*, 1989, **20**, 293.
22 J. O'M. Bockris and A. K. N. Reddy, *Modern Electrochemistry*, Plenum Press, New York, 1970.
23 D. Yates, S. Levine and T. W. Healy, *J. Chem. Soc., Faraday Trans. I*, 1974, **70**, 1807.
24 C. L. De Ligny, P. F. M. Luykx, M. Rehbach and A. A. Wieneke, *Recl. Trav. Chim. Pays Bas*, 1960, **79**, 699 and 713.
25 See references cited in ref. 20.
26 S. D. Moss, J. Janata and C. C. Johnson, *Anal. Chem.*, 1975, **47**, 2238.
27 G. Chaput, G. Jeminet and J. Juillard, *Can. J. Chem.*, 1975, **53**, 2240.
28 T. B. Stolwijck, L. C. Vos, E. J. R. Sudhölter and D. N. Reinhoudt, *Recl. Trav. Chim. Pays Bas*, 1989, **108**, 13.
29 J. P. Roger, C. Fretigny and T. Thami, in preparation.

Received in Montpellier, France, 11*th August* 1997;
Paper 7/08759D